Building Simulation 2003

Eighth International IBPSA Conference
Eindhoven, Netherlands
August 11-14, 2003

A COMPARATIVE ASSESSMENT OF FUEL CELL COGENERATION HEAT RECOVERY MODELS

Alex Ferguson[1], Ian Beausoleil-Morrison[1], V. Ismet Ugursal[2]
[1]CAMNET Energy Technology Center, Natural Resources Canada. Ottawa, Canada
[2]Dalhousie University, Halifax, Canada

ABSTRACT

Two dissimilar models capable of predicting the electrical and thermal performance of residential cogeneration fuel cell systems have been developed for use with the ESP-r building simulation program. The first model examines low temperature polymer electrolyte fuel cell (PEFC) systems, while the second model is better suited for the modelling of internally-reforming, high temperature solid oxide fuel cell (SOFC) systems. The models use different approaches to estimate the heat recovered from the fuel cell. To quantify the differences inherent in these approaches, the models were configured to represent equivalent PEFC systems and their predictions were compared at a variety of operating points. In this paper, the heat recovery models are briefly described, and a comparative assessment based on the simulation results is presented. Recommendations for the use of the models in studying cogeneration PEFC systems are also discussed.

INTRODUCTION

Fuel cell (FC) systems have received increasing attention in recent years as a viable alternative to meet the electrical and thermal needs of buildings. Operational fuel cell systems have demonstrated superior performance to combustion-based generation technologies at scales from 5kW to 2MW, a range that includes the electrical requirements of most buildings. Furthermore, fuel cells produce surplus heat suitable for space and domestic hot water heating. The US Department of Energy (2000) has published a detailed discussion of these systems and their operation.

Since fuel systems can convert 40% to 50% of the fuel's chemical energy to electricity (based on lower heating value), exploiting the thermal output can substantially improve the overall system efficiency. The utilization of this heat requires either coincident thermal and electrical demands, a system capable of effectively storing the fuel cell's thermal and/or electrical output, or the capacity to export electricity to the local utility grid. Therefore, building simulation is a valuable technology for studying these complex systems. (Beausoleil-Morrison et al. 2002)

In 2002, Ferguson and Ugursal (2002) published a parametric model for the study of polymer electrolyte fuel cell (PEFC) cogeneration systems. PEFC systems operate at low temperature (50–90 °C), and are fueled using hydrogen or natural gas that has been converted to a mixture of hydrogen and carbon dioxide. The hydrogen reacts with oxygen to produce water, which forms as a liquid due to the low operating temperature. The performance of PEFC systems is sensitive to the stack operating temperature, and may deteriorate by as much as 60% with deviations of 15 °C from the design operating temperature (Chalk 1996). The excess heat is recovered from PEFC systems by circulating cooling water through the fuel cell stack.

In the same year, Beausoleil-Morrison et al. (2002) also completed a solid oxide fuel cell (SOFC) modelling study using a generic cogeneration fuel cell model that they developed. SOFC systems operate at high temperature (900-1050 °C), and can be fueled with natural gas without the use of an external fuel processor. Heat can be recovered from SOFC systems by passing the high temperature exhaust gases through a gas-to-water heat exchanger.

The PEFC and generic FC models use different methods to determine the amount of heat that can be recovered from the fuel cell stack. In the generic FC model, an empirical relationship is used to evaluate the effectiveness of the heat exchanger, while the PEFC model assumes that all of the surplus heat in the stack can be recovered as long as a minimum temperature difference exists between the fuel cell stack and the cooling water.

In the present study, qualitative and quantitative analyses of the two heat recovery models were conducted using comparative testing. For this purpose, the models were modified to represent an equivalent PEFC system. This paper provides a brief overview of the ESP-r/HOT3000 simulation environment, for which both models were designed. The test case devised for this study is described, the models are discussed, and the modifications necessary to ensure that they represent the test case are detailed. The methodology used to compare the models is described, and the results are presented. Finally, conclusions are drawn about the use of the models in different PEFC simulation applications.

ESP-r/HOT3000 SIMULATION ENGINE

The fuel cell models used in this work were designed for use in the explicit HVAC modelling domain of the ESP-r/HOT3000 simulation engine. This simulator is based on the comprehensive and extensively validated ESP-r

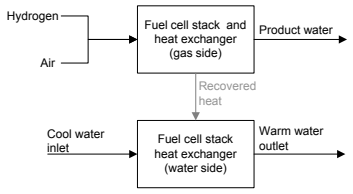

Figure 1: Simplified PEFC system

program developed at the University of Strathclyde, with algorithmic additions by the CANMET Energy Technology Centre (CETC) to support the modelling of Canadian (and international) housing. Clarke (2001) provides a thorough discussion of ESP-r's simulation methodologies, while Hensen (1991) describes the ESP-r explicit HVAC simulation domain.

Explicit HVAC domain

ESP-r/HOT3000's explicit HVAC modelling domain is based upon a component-level approach whereby users assemble components into a coherent HVAC system. Users must also specify how components are controlled, indicating what variables are sensed, and how components are actuated in response to the sensor signals. Each component in the HVAC network is represented by one of more control volumes and each control volume is characterized by mathematical models that describe the control volume's energy and mass exchanges with connected components and the environment. The energy balances are expressed in the following form:

$$MC_p \frac{\partial T}{\partial t} = \sum_{i=1}^{n} q_i \qquad (1)$$

where M is the mass of the control volume, C_p its heat capacity, T its temperature, t is time, and q_i is an energy flow into the control volume.

Matrices of equations that describe the HVAC network's thermal and mass flow state are formed using these energy and mass balances. A direct solution approach is used to solve these matrices, and because the equation set is non-linear, iteration is used to reform and resolve the matrices until convergence is achieved.

SIMPLIFIED TEST CASE

The arrangement of heat recovery equipment in SOFC and PEFC systems is fundamentally different. Whereas the electrochemical reactions in a SOFC stack occur at high temperatures (900-1050 °C) and produce a high temperature exhaust stream that is suitable for heat recovery, PEFC stacks perform best at comparatively low temperatures (80-90 °C) and require cooling to ensure optimum performance. In most cogeneration PEFC systems, the required cooling is achieved by circulating cooling water through manifolds in the stack.

To ensure that the model results would be comparable, the models were adapted to represent the simplified PEFC system depicted in Figure 1. This test case is comprised of a PEFC stack coupled to a heat exchanger, through which cooling water circulates.

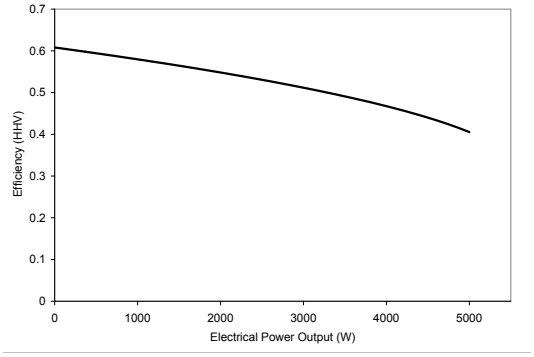

Figure 2: Test case part-load electrochemical performance

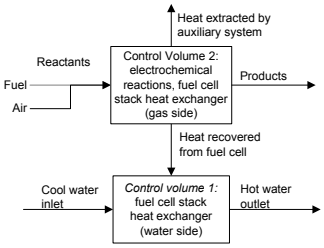

Figure 3: PEFC component model (Model A)

The stack is fueled with hydrogen and stoichiometric air at atmospheric temperature and pressure, which are assumed to react completely. The stack operates at 90 °C, and has a maximum gross electrical output of 5kW. The electrochemical characteristics of the test case are described by the arbitrary electrochemical efficiency profile plotted in Figure 2. In this study the behavior of auxiliary equipment, such as compressors, pumps, and heat rejection equipment was not considered.

PEFC MODEL (MODEL A)

The PEFC model, henceforth referred to as *Model A*, was published by Ferguson & Ugursal (2002). It consists of (1) an electrochemical model that predicts the behavior of the fuel cell stack, (2) thermodynamic models that predict the behavior of the reactors in the fuel processor, and (3) auxiliary system models that predict the behavior of other systems such as compressors, pumps and heat rejection equipment. Ferguson (2003) provides a detailed discussion of the development and validation of this model.

For this study, Model A was modified to consider the simplified test case. The water side of the PEFC stack heat exchanger was represented using a single control volume, while the electrochemical and thermal processes occurring on the gas side of the fuel cell stack heat exchanger were modelled using another control volume. This arrangement is depicted in Figure 3.

First control volume

The first control volume in Model A represents the water side of the fuel cell stack heat exchanger. The energy

balance for this control volume is as follows:

$$\dot{m}C_p(T_{cw_o} - T_{cw_i}) = \dot{Q}_{rec.} \quad (2)$$

where $\dot{m}$ is the flow rate of the cooling water entering the heat exchanger, C_p is the specific heat of the cooling water, and T_{cw_i} and T_{cw_o} are the temperature of the cooling water entering and exiting the control volume, respectively. The term $\dot{Q}_{rec.}$ represents the amount of heat recovered from the fuel cell, and will be described shortly.

Second control volume

The second control volume in Model A considers the electrochemical and thermal processes occurring on the gas side of the fuel cell stack. The total amount of chemical energy released in the fuel cell stack is quantified by the change in enthalpy that occurs inside the stack (ΔH_{stack}):

$$\begin{aligned} \Delta H_{stack} &= \sum_{i=1}^{reactants} \left(\dot{N}(h_f + h_T - h_{STP}) \right)_i \\ &- \sum_{j=1}^{products} \left(\dot{N}(h_f + h_T - h_{STP}) \right)_j \end{aligned} \quad (3)$$

where for a given species, $\dot{N}$ is the flow rate, h_f is the enthalpy of formation at standard temperature and pressure, h_T is the enthalpy at temperature T and h_{STP} is the enthalpy at standard temperature and pressure.

The amount of electrical work produced by the fuel cell stack ($\dot{W}_{elec.}$) is determined using the total change in enthalpy occurring in the fuel cell stack and the overall efficiency (η_{stack}). The chemical energy released in the fuel cell stack that is not converted to electric work is converted into heat ($\dot{Q}_{stack}$):

$$\dot{W}_{elec.} = \eta_{stack}\Delta H_{stack} \quad (4)$$

$$\dot{Q}_{stack} = \Delta H_{stack} - \dot{W}_{elec.} \quad (5)$$

A parametric relationship is used to describe the efficiency of the fuel cell stack as a function of its electrical power output. The development of this relationship has been described previously by Ferguson and Ugursal (Ferguson & Ugursal 2002, Ferguson 2003).

Since the performance of PEFC systems is dependent on the operating temperature, the heat produced in the fuel cell stack ($\dot{Q}_{stack}$) must be extracted to ensure efficient operation. Heat may be transferred from the fuel cell stack by three mechanisms: (1) heat can be transferred to the cooling water flowing through the fuel cell stack ($\dot{Q}_{rec.}$), (2) heat may be transferred from the high temperature stack to the cooler surroundings by convection and radiation ($\dot{Q}_{loss}$), and (3) heat may be extracted using an auxiliary heat rejection system ($\dot{Q}_{rej.}$), if such a system is present.

$$\dot{Q}_{stack} = \dot{Q}_{rec.} + \dot{Q}_{loss} + \dot{Q}_{rej.} \quad (6)$$

Since the PEFC system in the test case operates adiabatically, the heat loss from the stack was set to zero.

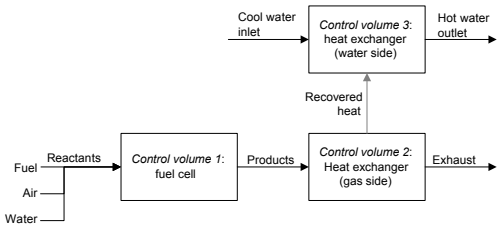

Figure 4: SOFC component model (Model B)

Model A assumes that all of the surplus heat available in the fuel cell will be transferred to the cooling water as long as a minimum temperature difference $\Delta T_{min.}$ exists between the cooling water and the fuel cell stack. Thus, there exists a maximum amount of heat that can be transferred to the cooling water while maintaining the minimum temperature difference:

$$\dot{Q}_{max.} = \dot{m}_{cw}C_p\left((T_{stack} - \Delta T_{min.}) - T_{cw_i}\right) \quad (7)$$

$$\dot{Q}_{rec.} = \begin{cases} \dot{Q}_{stack} & \text{if } \dot{Q}_{max.} \geq \dot{Q}_{stack} \\ \dot{Q}_{max.} & \text{if } \dot{Q}_{max.} < \dot{Q}_{stack} \end{cases} \quad (8)$$

where $\dot{Q}_{stack}$ is the surplus heat available in the fuel cell stack and $\dot{Q}_{max.}$ is the maximum amount of heat that can be transferred between the fuel cell stack and the cooling water. If the amount of heat recovered is less than the surplus heat available, Model A assumes that the unrecovered surplus heat will be extracted using an auxiliary heat rejection system (ie. $\dot{Q}_{rej.} = \dot{Q}_{stack} - \dot{Q}_{rec.}$) to ensure that the optimal operating temperature is maintained. In the PEFC model published by Ferguson and Ugursal, the performance of the cooling equipment is estimated using a parametric equation. However, in the present study the behavior of this cooling system is not considered. The determination of $\Delta T_{min.}$ will be discussed shortly.

GENERIC FC MODEL (MODEL B)

The generic FC model, henceforth referred to as *Model B*, was published by Beausoleil-Morrison et al. The model is comprised of three separate control volumes, which are depicted in Figure 4. The first control volume represents the fuel cell, while the second and third control volumes represent the exhaust-to-water heat exchanger: control volume two corresponds to the gas side of the heat exchanger while control volume three represents the water side. Beausoleil-Morrison et al. (2002) provide a complete description of the model and its application.

Model B was modified to consider the simplified test case by using the first and second control volumes two to jointly represent the reactant and product gases flowing through PEFC stack, and the third control volume to represent the cooling water flowing through the fuel cell stack. This configuration is depicted in Figure 5.

In Model B, the electrochemical reactions are assumed to occur in the first control volume. A substantial amount of heat is produced as a result of inefficiencies in the fuel

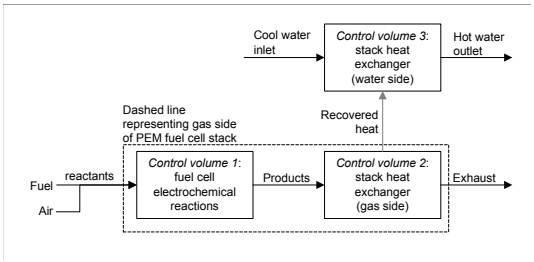

Figure 5: Adaptation of Model B to represent PEFC stack

cell stack, and, in a real PEFC stack, this heat is transferred directly from the fuel cell stack electrodes to the cooling water. However, Model B assumes that this heat is transferred to the product gases of the electrochemical reaction, raising their temperature. In the second control volume, the high temperature product gases undergo sensible cooling and the heat produced in the fuel cell stack is transferred to the cooling water.

The high temperature exhaust gases exiting the first control volume in Model B do not exist in real PEFC stacks, where excess heat is directly transferred to the cooling water as it is released in the electrochemical reactions. However, if these high temperature gases are cooled to the fuel cell stack operating temperature in the second control volume, the amount of heat recovery estimated by Model B will reflect the actual heat transferred from a PEFC stack to the cooling water. Thus, Model B may be used to represent PEFC stacks if the model is configured such that the predicted exhaust gas temperature is within the normal range of operation for this type of fuel cell.

First control volume

The first control volume energy balance is as follows

$$\sum_{i=1}^{reactants} (\dot{N}h)_i + \phi_{chemical} = \sum_{k=1}^{products} (\dot{N}h)_k + \dot{W}_{elec.} + \dot{Q}_{loss} \quad (9)$$

where $\phi_{chemical}$ represents the rate at which chemical energy is supplied to the fuel cell, $\dot{W}_{elec.}$ is the net electrical output of the fuel cell system, and $\dot{Q}_{loss}$ represents the heat lost from the fuel cell stack to the room containing the fuel cell. The first term on the left hand side of Equation 9 represent the rate that enthalpy associated with the reactant streams enters the control volume, while the first term on the right hand side represents the rate that enthalpy associated with the product stream leaves of the control volume.

Since the product water forms as a liquid in PEFC systems, the rate at which chemical energy is supplied to the fuel cell ($\phi_{chemical}$) is evaluated based on the higher heating value (HHV) of the fuel:

$$\phi_{chemical} = \sum_{i=1}^{fuel} (\dot{N} \cdot HHV)_i = \dot{N}_{fuel} \cdot HHV_{fuel} \quad (10)$$

The net electrical output of the fuel cell depends on the rate of chemical energy supplied to the fuel cell and its overall electrical efficiency (HHV):

$$\dot{W}_{elec.} = \eta_{elec.} \cdot \phi_{chemical} \quad (11)$$

where $\eta_{elec.}$ represents the overall electrical conversion efficiency of the fuel cell system, and is evaluated using a parametric relationship describing the efficiency as a function of the electrical output.

The final term in Equation 9, $\dot{Q}_{loss}$, represents the heat lost to the fuel cell's surroundings. Since the PEFC system in the test case is assumed to operate adiabatically, the heat loss from the stack was set to zero for this study.

Second control volume

The energy balance for the second control volume, representing the gas side of the heat exchanger, is given by:

$$\sum_{k=1}^{products} (\dot{N}h)_k = \sum_{l=1}^{exhaust} (\dot{N}h)_l + \dot{Q}_{rec.} \quad (12)$$

The left hand side of Equation 12 represents the rate at which enthalpy is carried into the control volume by the hot product gases exiting the first control volume. The first term on the right hand side represents the rate at which enthalpy is carried out of the second control volume by the rejection of cool exhaust.

The last term in Equation 12 ($\dot{Q}_{rec.}$) represents the heat transferred from the hot product gases to the water in the heat exchanger, and quantifies the fuel cell's thermal output. The amount of heat transfer is evaluated using the temperatures of the product gases ($T_{products}$) and water (T_{cw_i}) at the inlets of the heat exchanger, and an effective heat transfer coefficient ($UA_{eff.}$):

$$\dot{Q}_{rec.} = UA_{eff.} \cdot (T_{products} - T_{cw_i}) \quad (13)$$

The flow rate of the cooling water through the fuel cell stack is the significant factor in determining the overall heat transfer coefficient between the fuel cell stack and the cooling water. Model B uses a heat exchanger effectiveness approach to determining the overall heat transfer coefficient between the high temperature gases and cooling water:

$$UA_{eff.} = \varepsilon C_{min} \quad (14)$$

where C_{min} represents the heat capacity (W/°C) of the product gases or the cooling water, whichever is smaller, and ε is a dimensionless coefficient ($0 \leq \varepsilon \leq 1$) quantifying the effectiveness[1] of the heat recovery facilities. The coefficient ε is evaluated as a function of the cooling water volumetric flow rate using a parametric relationship:

$$\varepsilon = \theta_0 + \theta_1 \cdot \dot{V}_{water} + \theta_2 \cdot \dot{V}_{water}^2 \quad (15)$$

[1] Since the temperature difference between the product gases and the cooling water in Model B is much higher than the temperature difference driving heat recovery in a PEFC stack, the effectiveness ε used to configure Model B is not representative of an actual PEFC stack heat exchanger.

Table 1: Model A Configuration

Parameter	Value
Maximum electrical output (W)	5000
Fuel composition	100% H_2
Stack operating temperature ($^\circ$C)	90
Minimum heat recovery temperature - difference $\Delta T_{min.}$ ($^\circ$C)	13.07

Table 2: Model B Configuration

Parameter	Value
Maximum electrical output (W)	5000
Fuel composition	100% H_2
Heat recovery coefficient θ_0	0
Heat recovery coefficient θ_1	6.609
Heat recovery coefficient θ_2	-8.639×10^{-5}

where $\dot{V}_{water}$ is the volumetric flow rate (l/s) of the cooling water entering the fuel cell, and coefficients θ_0, θ_1 and θ_2 are user inputs. The determination of θ_0, θ_1 and θ_2 will be discussed shortly.

Third control volume

The energy balance for the third control volume, representing the water side of the heat exchanger, is the same as the energy balance for the first control volume in Model A, and is described by Equation 2:

$$\dot{Q}_{rec.} = \dot{m}C_p(T_{cw_o} - T_{cw_i})$$

CONFIGURATION OF MODELS

Selected parameters used to configure the models are presented in Tables 1 and 2.

Electrochemical efficiency

Models A and B were configured to represent the part-load electrical efficiency profile depicted in Figure 2. When compared, the electrochemical efficiency predictions made by the two models differed by an average of 0.0040% and a maximum of 1.25% over the operating range. Therefore, the models are assumed to predict the same electrochemical performance and thermal production at any given operating point.

Heat recovery

The heat exchanger effectiveness coefficients θ_0, θ_1 and θ_2 required by Model B were determined by assuming that under a set of design conditions[2], (1) the temperature of the second control volume in Model B (ie. the outlet temperature of the product gases) is equal to the stack design operating temperature (90 $^\circ$C), and (2) the part load characteristics of the heat exchanger are similar to the heat exchanger characteristics used in another fuel cell modelling study (Beausoleil-Morrison et al. 2002). Thus, the values of θ_0, θ_1 and θ_2 (presented in Table 2) obtained using these criteria represent an arbitrary, but realistic PEFC heat recovery system. Under the design conditions, the effectiveness value obtained using these coefficients approaches 1.0, and nearly all of the surplus heat available in the fuel cell is transferred to the cooling water.

[2] $\dot{W}_{elec.}$ = 5000W, T_{cw_i} = 65 $^\circ$C, $\dot{V}_{cw}$ = 0.15 l/s

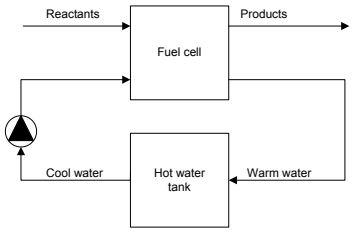

Figure 6: Mechanical plant arrangement

The minimum temperature difference parameter $\Delta T_{min.}$ required by Model A was determined by first using Model B to predict the amount of heat recovered under the design conditions. Then the minimum temperature difference $\Delta T_{min.}$ value that resulted in the same heat recovery estimate in Model A under the same conditions was determined using an iterative approach. This value is presented in Table 1.

SIMULATION

Each model was integrated into the mechanical plant model depicted in Figure 6. In this arrangement, a pump draws water from the hot water tank and circulates it through the fuel cell, where it is heated. The water is then returned to the hot water tank.

The temperature inside the hot water tank may effect the heat recovery estimates made by the models, and must be controlled to ensure that model results are comparable. A 29.3 kW gas burner is attached to the hot water tank, and can be turned on and off as required to maintain the temperature between upper and lower set points. The heat produced by the fuel cell may also raise the temperature of the tank. Therefore, the temperature inside the hot water tank can be maintained between two set points if (1) the time resolution of the simulation is small enough to allow the burner to be turned on or off before the temperature falls below or exceeds the set points, and (2) the thermal load on the hot water tank is always greater than the fuel cell's thermal output, so that the fuel cell cannot raise the temperature of the tank above the upper setpoint.

These criteria were satisfied by increasing the mass of the hot water tank to 2000kg so that the burner would require several minutes to increase the temperature of the tank by 1 $^\circ$C. The thermal load on the hot water tank was increased by specifying an overall hot water tank heat loss coefficient of 300W/ $^\circ$C, which provides a heat loss from the tank of 9kW when there is a 30 $^\circ$C temperature difference between the hot water tank and the surroundings. This is larger than the maximum thermal output of the fuel cell system ($\sim$7.3kW at full power).

Operation of the gas-fired burner was managed using a control loop that activates the burner when the temperature drops below a lower set point, and deactivates the

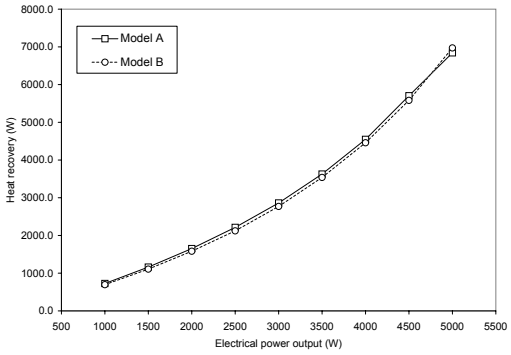

Figure 7: Model heat recovery estimates under design conditions (T_{cw_i} = 65 °C, $\dot{V}_{cw}$ = 0.15 l/s)

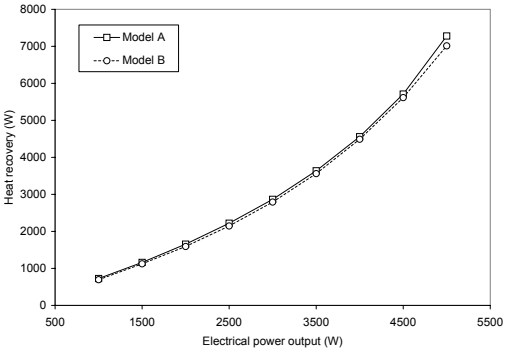

Figure 8: Model heat recovery estimates at reduced cooling water inlet temperature (T_{cw_i} = 55 °C, $\dot{V}_{cw}$ = 0.15 l/s)

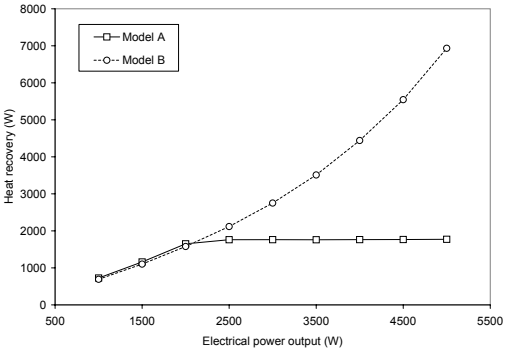

Figure 9: Model heat recovery estimates at increased cooling water inlet temperature (T_{cw_i} = 74 °C, $\dot{V}_{cw}$ = 0.15 l/s)

burner when the temperature rises above a upper set point. Since the tank has a large thermal mass, the controller can maintain the tank temperature between the upper and lower set points even when the difference between the set points is less than 1 °C, as long as the time resolution of the simulation is sufficiently small[3]. Thus, this configuration permits control of the temperature of the hot water tank, and therefore the cooling water inlet temperature, to within a fraction of a degree centigrade.

The response of the heat recovery estimates made by Models A and B to variations the cooling water inlet temperature was observed by conducting simulations using the design flow rate of 0.15 l/s and a range of temperatures between 55 °C and 74 °C. The response of the heat recovery estimates to variations the cooling water flow rate was observed by conducting simulations using the design inlet temperature of 65 °C and a range of flow rates between 0.13 l/s and 0.17 l/s. In each simulation, the behavior of the fuel cell was characterized over its full range of operation (1kW–5kW).

RESULTS

Heat recovery estimates

The heat recovery predictions made by Models A and B for the design conditions are plotted in Figure 7. The data show excellent agreement; the estimates differ by an average 3% and a maximum of 7.2%. Figure 8 shows the heat recovery predictions when the cooling water inlet temperature is decreased to 55 °C. Again the estimates agree well, differing by an average of 2.8% and a maximum of 4.6%. Figure 9 shows the heat recovery predictions when the cooling water inlet temperature is increased to 74 °C. Under these conditions, the model predictions agree well at power levels below 40% of full power, but the disparity between the estimates grows as power is further increased.

While a reduction the cooling water inlet temperature should result in and increase in the amount of heat recovery estimated by Model A (see Equations 7 and 8) there is little difference in the Model A estimates plotted in Figures 7 and 8. The amount of heat recovery ($\dot{Q}_{rec.}$) predicted by Model A at the design conditions is nearly equal to the amount surplus of heat produced in the fuel cell ($\dot{Q}_{stack}$). Thus, decreasing the inlet temperature does not result in significantly higher amounts of heat recovery.

Conversely, increasing the cooling water inlet temperature has a significant impact on the heat recovery predictions of Model A. Increasing the inlet temperature reduces the maximum amount of heat that can be transferred to the cooling water while still maintaining the specified minimum temperature difference between the cooling water and the fuel cell stack (see Equation 7). If the available heat ($\dot{Q}_{stack}$) exceeds the maximum amount of heat that can be transferred to the cooling water ($\dot{Q}_{max.}$), Model A assumes that the surplus heat will be extracted using an auxiliary heat rejection system to ensure that the fuel cell stack is maintained at its optimal operating temperature. As a result, Model A predicts the same amount of heat recovery ($\dot{Q}_{max.}$) for all operating points at which the amount of heat available in the fuel cell is equal to or greater than $\dot{Q}_{max.}$, and this behavior is illustrated in Figure 9. Above 2kW electrical output, Model A assumes that additional produced in the fuel cell system heat cannot be transferred to the cooling water.

Figures 7–9 show that the heat recovery estimates of Model B are generally insensitive to changes in the cooling water inlet temperature. The temperature difference between the product gases (ie. the temperature of control volume one) and the cooling water inlet temperature

[3] A one-minute time step provided adequate control of the hot water tank temperature in this configuration.

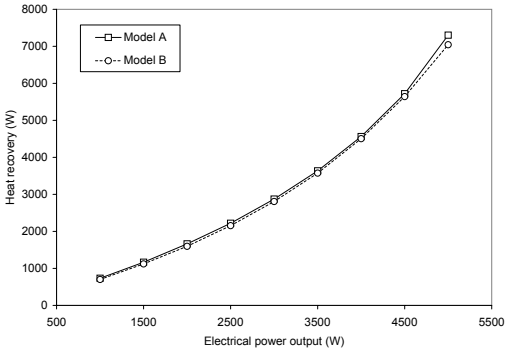

Figure 10: Model heat recovery estimates at increased cooling water flow rate (T_{cw_i} = 65 °C, $\dot{V}_{cw}$ = 0.17 l/s)

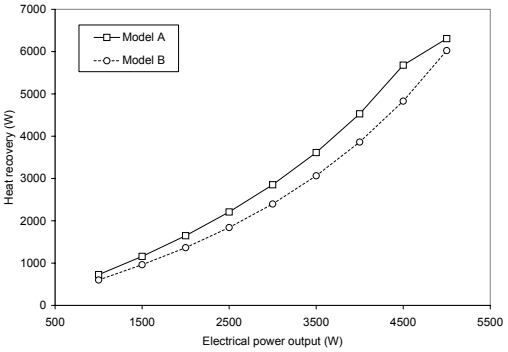

Figure 11: Model heat recovery estimates at reduced cooling water flow rate (T_{cw_i} = 65 °C, $\dot{V}_{cw}$ = 0.13 l/s)

may vary from 1600 °C to 2400 °C over the operating range. Since this temperature difference is used to determine the amount of heat that can be recovered (Equation 13), variations of 20 °C or more in the cooling water inlet temperature have little impact on the model heat recovery estimates.

Figure 10 shows the heat recovery predictions made by Models A and B when the cooling water volumetric flow rate is increased to 0.17 l/s. The estimates agree well, differing by an average of 2.7% and a maximum of 4.6%. Figure 11 shows the heat recovery predictions when the cooling water flow rate is decreased to 0.13 l/s. Under these conditions, the model predictions differ by an average of 17% and a maximum of 22%.

In Model A, the maximum amount of heat that can be transferred to the cooling water while maintaining the minimum temperature difference is proportional to the cooling water flow rate (see Equation 7). However, the heat recovery estimates of Model A were only effected by variations in the cooling water flow rate at the maximum power output (5kW). Below this operating point, the available heat ($\dot{Q}_{stack}$) was less than the maximum heat that can be transferred to the cooling water ($\dot{Q}_{max.}$) and the estimated heat recovery was the same over the range of volumetric flow rates considered in this analysis.

In Model B, the effectiveness of the heat exchanger is determined as a function of the cooling water volumetric flow rate (see Equation 15). However, under the design conditions the effectiveness of the heat exchanger is above 99%, and almost all of the surplus heat produced in the fuel cell is transferred to the cooling water. Thus, further increasing the volumetric flow rate does not yield significant increases in the heat recovery estimates, and the heat recovery estimates made by Models A and B agree well at elevated flow rates.

Conversely, decreasing the cooling water flow rate results in a reduction in the heat exchanger effectiveness calculated by Model B, and a corresponding reduction in the estimated heat recovery. Thus, the heat amount of heat recovery estimated by Model B was significantly lower than that predicted by Model A at a volumetric flow rate of 0.13 l/s, as shown in Figure 11.

Exhaust gas temperature

Figure 12 depicts the exhaust temperature estimated by Model B for a range of cooling water inlet temperatures between 55 °C and 74 °C. While changes in the inlet temperature do not significantly effect the heat recovery estimated by Model B, they are accompanied by a corresponding change in the exhaust gas outlet temperature.

In Figure 13, the response of the Model B exhaust gas temperature estimates to variations in the cooling water flow rate is plotted. When the cooling water flow rate is reduced by 7% to 0.14 l/s, the fuel cell exhaust gas outlet temperature at full power reaches 297 °C, which is well above the operating range of PEFC fuel cell stacks. Further decreasing the cooling water flow rate results in even higher fuel cell stack operating temperatures. Therefore, it is not practical to operate the system at cooling water flow rates below the design flow rate.

In operating PEFC systems, stack temperature variations of 15-20 °C might result in a reduction in electrochemical performance of more than 60% (Chalk 1996). Since neither model considers the effects of temperature on the stack efficiency, the stack temperature predicted by the models must be maintained within the design operating range to ensure the results are accurate. As Model B permits the estimated stack temperature to float depending on conditions in the heat exchanger, it must be coupled to models representing an auxiliary heat rejection system and its associated controls to ensure that the predictions of Model B remain inside the normal operating range.

General remarks

These results illustrate a fundamental difference between Models A and B. Whereas Model B permits the fuel cell stack operating temperature to float depending on the fuel cell operating point and the conditions on the water side of the heat exchanger, Model A assumes that the fuel cell stack operating temperature must be maintained at the user-specified value to ensure efficient operation. If the surplus heat in the fuel cell stack cannot be transferred to the cooling water while maintaining the specified minimum temperature difference, Model A assumes that the

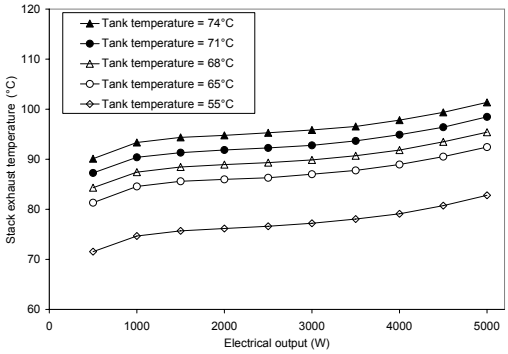

Figure 12: Model B exhaust gas outlet temperature response to changes in the cooling water inlet temperature

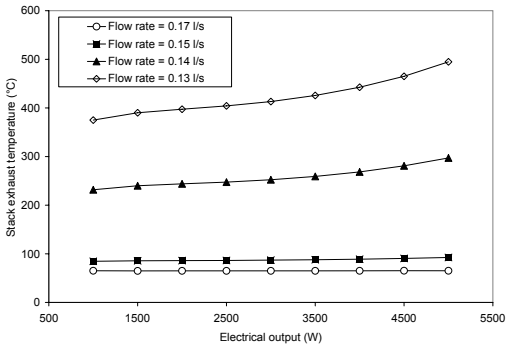

Figure 13: Model B exhaust gas outlet temperature response to changes in the cooling water flow rate

unrecovered surplus heat will be extracted from the stack using other means.

CONCLUSIONS

Two dissimilar models were adapted to represent a simplified PEFC fuel cell system and their results were compared. The model heat recovery estimates show reasonable agreement when the cooling water inlet temperature is below the design inlet temperature and the cooling water volumetric flow rate is above the design flow rate with which the models were configured. The results suggest that the models can be used with confidence in this region. Outside of this region, differences between the treatment of the fuel cell operating temperature in the models produce substantial disparity in the model estimates.

Model A assumes that the fuel cell stack must be maintained at its specified operating temperature, and that unrecovered surplus heat will be extracted using auxiliary heat rejection equipment. The original PEFC model on which Model A is based used a simple parametric relationship to predict the performance of this equipment.

However, Model B permits the fuel cell operating temperature to float and, depending on the conditions in the fuel cell stack heat exchanger, may predict fuel cell stack temperatures outside of the system operating range. Therefore, detailed models of the auxiliary heat rejection equipment and associated controls used to regulate the fuel cell stack operating temperature are also necessary to use Model B in a PEFC cogeneration modelling study. Detailed models of these systems would also permit the interactions between the fuel cell and heat rejection systems to be studied.

Based on these results, Model A is recommended for low-resolution PEFC modelling studies in which detailed modelling of the auxiliary cooling equipment is unnecessary. Model B is recommended for higher-resolution studies when the interactions between the fuel cell stack, water tank and heat rejection equipment are of interest.

This study also highlights the factors requiring consideration during inter-model comparative testing. This is a powerful method commonly used to validate algorithms in building simulation programs (Judkoff & Neymark 1995), but significant effort is required to devise test cases and ensure that they are accurately represented.

REFERENCES

Beausoleil-Morrison, I., Cuthbert, D., Deuchars, G. & McAlary, G. 2002. , The simulation of fuel cell cogeneraion systems within residential buildings, 'Proc. of eSim, bi-annual conf. of IBPSA-Canada', IBPSA-Canada.

Chalk, S. 1996 , Research and Development of Proton-Exchange-Membrane (PEM) fuel cell system of Transportation Applications, Allison Gas Turbine Division, General Motors Corporation.

Clarke, J. 2001 , Energy simulation in building design, second edn, Butterworth Heinemann.

Ferguson, A. 2003. , Fuel cell modelling for building cogeneration applications, Master's thesis, Dalhousie Univ., Halifax, Canada.

Ferguson, A. & Ugursal, V. 2002. , A fuel cell model for building cogeneration applications, 'Proc. of eSim, bi-annual conf. of IBPSA-Canada', IBPSA-Canada.

Hensen, J. 1991. , On the thermal interaction of building structure and heating and ventilation system, PhD thesis, Eindhoven Univ. of Technology.

Judkoff, R. & Neymark, J. 1995. , International energy agency building energy simulation test (BESTEST) and diagnostic method, Technical report, National Renewable Energy Laboratory, US Department of Energy.

US Department of Energy 2000 , Fuel Cell Handbook, Fifth Edition, National Energy Technology Laboratory, US Department of Energy.